Author Accepted Manuscript version of the paper by Hagar Elarga et al.
in Proceedings of the 26th IIR International Congress of Refrigeration: Paris , France, August 21-25, 2023 - volume 4 (2023) p. 1105-1116,
http://dx.doi.org/10.18462/iir.icr.2023.0457

DOI: 10.18462/iir. 10.18462/iir.icr.2023.0457

Innovative reheat approach of the TES system during the hotel's standstill operation utilizing a CO_2 heat pump unit

Hagar ELARGA*[(a)], Ángel Á. PARDIÑAS [(b)], Silvia MINETTO[(c)], Armin HAFNER[(d)]

[(a)] **SINTEF Energy Research,**
Trondheim, 7465, Norway
[(b)] **Technological Institute of Galicia Foundation**
A Coruña, 15003, Spain
[c)] **CNR Italian National Research Council,**
Padua, 35127, Italy
[d)] **NTNU Norwegian University of Science and Technology,**
Trondheim, 7491, Norway
***Corresponding author:** hagar.elarga@sintef.no

ABSTRACT

The implementation of CO_2 as a refrigerant is considered one of the solutions to improve the overall building's energy performance, especially if the heat recovery concept is applied. In this paper, an innovative approach to compensate for the thermal losses of the in-series stratified thermal energy storage (TES) tanks during periods with insignificant Domestic Heating Water (DHW) demands is numerically investigated using Modelica language. The approach adopts a CO_2 heat pump/chiller unit with two water-cooled gas coolers and an air-cooled gas cooler in the case of cooling only is required. The flow leaving one of the middle tanks is mixed with the flow leaving the first gas cooler and the mixture is heated up through the second gas cooler to the heating setpoint and circulated back to the TES system. Results have shown improvements in the thermal charging efficiency, while the system COP has reached 5.5 compared to 4.4 if the reheating approach is not adopted. TIL, Modelica Buildings, and Modelica standards libraries were used to develop the model.

Keywords: Thermal Energy Storage, CO_2, Heat Pump, chiller, Modelica

1. INTRODUCTION

CO_2 vapor compression systems could be utilized in heating, cooling, and refrigeration applications, which opens the research door to investigate several design aspects. Due to its low critical temperature, the transcritical CO_2 cycle is generally applied (Lorentzen and Pettersen, 1993), and recent studies have demonstrated the enormous energy-saving potential of implementing a transcritical CO_2 system (Dai et al., 2020b). Especially for the water heating application (Ye et al., 2022) with a significant temperature lift, the transcritical CO_2 cycle presents a unique superiority compared to traditional HFC refrigerants (Austin and Sumathy, 2011). Cui et al. (2022) highlighted that the pinch point in the gas cooler significantly impacts the optimal discharge pressure and system performance of the CO_2 heat pump water heater. For that, a thermodynamic model was developed and validated, and a faster and more effective method for seeking optimal discharge pressure was proposed and proven accurate. In addition to all its environmental gains, R744 could be promoted as a single-unit refrigerant, meaning it can simultaneously meet the required building refrigeration cooling and heating requirements (Pardiñas et al., 2018). Minetto et al. (2016) described the development of a reversible heat pump for space heating and cooling based on a CO2 transcritical cycle, which aims to recover the expansion work loss using a two-phase ejector. The experimental assessment of the heating and cooling mode operations was reported to maintain satisfactory values for COP and energy efficiency ratio under the capacity of the proposed layout to operate as a heat pump and chiller.

Elarga and Hafner (2023) have numerically compared the thermal and energy performance of a heat pump/chiller unit with and without heat recovery for an office building in three different cities in the summer season. Results have demonstrated that COP values for heat recovery and hotter climates are much higher than colder climates. Yamaguchi et al. (2011) have developed and validated a simulation model for a CO2 heat pump water heater of 22.3 kW. In simulations and experiments, the effects of the inlet water temperature and outside air temperature on the system characteristics were discussed. As a result, the average difference in COP between the simulation and experimental results was recorded as 1.5%. Elarga and Hafner (2022) have proposed a CO2 heat pump chiller unit with a thermal energy storage (TES) system for a hotel in India to replace a conventional chiller and separate boiler system with a COP equal to 3. Numerical results have shown an increment in COP that reached 6.7 and 5.7 if the circulating pumps are considered. Smitt et al. (2020) have numerically investigated the TES of a hotel's CO2 heat pump/chiller system. The authors proved that charging at reduced loads has the potential to limit return temperatures from the secondary systems and, by this, enhance system performance. Smitt et al. (2021) have theoretically compared the energy consumption, environmental impact, and cost of three different design concepts for integrated CO2 units equipped with thermal storage. Results have shown that ejector-supported parallel compression was superior regarding the annual COP, investment cost, and electricity prices.

The current numerical study proposes a simple yet innovative scheme to reheat the TES system, especially during periods with low or no heating demands, adopting a CO_2 heat pump/chiller unit with two water-cooled gas coolers and an air-cooled gas cooler in the case of cooling only is required. The flow leaving one of the middle tanks is mixed with the flow leaving the second gas cooler and heated up to the heating setpoint, and circulated back to the TES system. Moreover, the study includes a comparative analysis between two cases of the TES system, with and without the innovative reheating approach. This comparison highlighted the induced differences in energy consumption and system performances.

2. METHODOLOGY

The system's main components include a CO_2 heat pump chiller unit with two in-series gas coolers, two in-series evaporators, two compressors, five in-series stratified TES tanks, and two variable frequency water pumps for chilled and heating water, respectively. Utilizing Modelica as a programming language and Dymola as a simulation environment, models were developed using different libraries: open source as the Modelica buildings library (MBL - V9.0.0) and Modelica standard library (MSL -V3.2.3) and the commercial library TIL 3.9.1. The model ran for five consecutive days from the first of August using the Dassl solver and $1e^{-4}$ tolerance. The effects of oil and oil management system are neglected.

2.1. System description

2.1.1. CO_2 heat pump chiller unit

The idea behind the current design of the CO_2 heat pump/chiller unit, as shown in Fig. 1, is to guarantee a system that performs efficiently in diverse operational modes. Accordingly, the compressor(s) set consists of two compressors, a variable frequency compressor varFCom, and a constant frequency compressor conFCom. Table 1 illustrates the nominal displacement volume capacities of the two compressors. The unit heat sink is divided into two parallel paths where the hot vapor leaving the compressors is either directed to the two in-series gas coolers GC (2 and 2') tube and tube type with a heat transfer area of 16 m^2 each or the second path with an air-cooled plate heat exchanger type PHX GC(2'') with a heat transfer area equal to 15 m^2. The heat sink path depends on the building's thermal requirements and the TES system status.

The high-pressure level is controlled via the ejector (4). The ejector's delivery port is connected to the low-pressure receiver (6), where it collects the gas/liquid mixture. Subsequently, the liquid stream leaving the bottom of the receiver is connected to leaving the evaporator (5) and flows through the evaporator back to the receiver by natural circulation (Artuso et al., 2021). Meanwhile, the other liquid stream connection expands to the evaporator (5') pressure setpoint. Whereafter, the refrigerant leaving (evaporator5') is connected to the ejector's suction port. Evaporator (5') design saturated pressure equals 40 bar, which is

Author Accepted Manuscript version of the paper by Hagar Elarga et al.
in Proceedings of the 26th IIR International Congress of Refrigeration: Paris , France, August 21-25, 2023 - volume 4 (2023) p. 1105-1116,
http://dx.doi.org/10.18462/iir.icr.2023.0457

maintained by controlling the frequency of the variable frequency compressor varFCom. An internal heat exchanger is installed upstream of the compressors' inlet manifold. It exchanges heat with the high-pressure side to guarantee superheated refrigerant arriving at the compressors' suction ports. A safety operation measurement is incorporated, which allows the control system to forcefully switch off the unit if the water entering GC2' is higher than 34 ˚C plus the hysteresis. This condition is to maximize the system's efficiency.

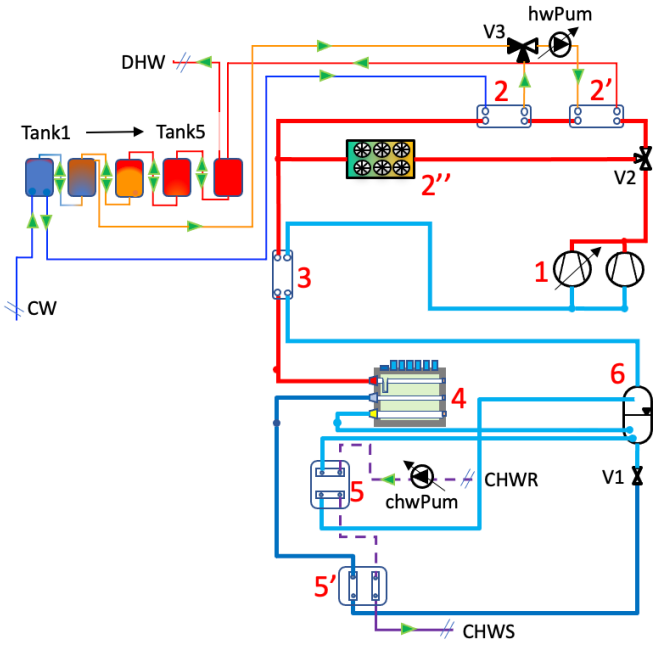

Figure 1: heat pump chiller unit thermal storage system layout

Table 1. Compressors set nominal capacities

Compressor	varFC		conFC
Frequency	30Hz	70Hz	50Hz
Swept volume per unit time ($m^3 \cdot h^{-1}$)	5.7	13.5	3.3

2.1.2. Two-phase flow ejector

In this section, a brief illustration of the ejector work concept and governing equations are presented. As shown in Fig. 2, the ejector is a component that can recover part of the system expansion work by converting the pressure energy into kinetic energy. It includes three main parts, the driving nozzle, where the increment in the kinetic energy of the high-pressure refrigerant flow due to cross-sectional area contraction creates a pressure drop. This allows the suction flow rate (SFR) to enter and mix with the driving flow rate (DFR) at the mixing chamber i.e. the second part. Subsequently, the refrigerant's mix enters the diffuser, i.e., the third part where the kinetic energy is converted into potential energy or pressure head over the suction pressure level, and it flows into the receiver.

Author Accepted Manuscript version of the paper by Hagar Elarga et al.
in Proceedings of the 26th IIR International Congress of Refrigeration: Paris , France, August 21-25, 2023 - volume 4 (2023) p. 1105-1116,
http://dx.doi.org/10.18462/iir.icr.2023.0457

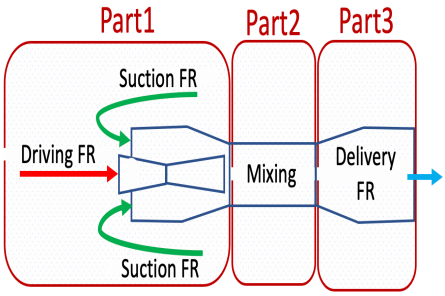

Figure 2: Two-phase flow ejector scheme

The physical definition of ejector efficiency quantifies the recovered expansion work, i.e., the ratio between the compression work of the evaporator flow to reach the delivery pressure level to the isentropic/isenthalpic expansion work of the GC flow from the high side pressure to the same delivery pressure level. While the mathematical definition Eq. (1) is derived as the ratio between the recovered expansion work $ExpW_{Rec}$ to the maximum possible recovery potential $ExpW_{Max}$

$$\eta_{eje} = x.\frac{ExpW_{rec}}{ExpW_{Max}} \qquad \text{Eq. (1)}$$

where x is the entrainment ratio, which is the ratio of the suction nozzle to the driving nozzle flow rate (kg/s), respectively as defined in Eq. (2).

$$x = \frac{\dot{m}_{Suc}}{\dot{m}_{Dri}} \qquad \text{Eq. (2)}$$

where $ExpW_{Rec}$ is the recovered expansion work and defined as the difference between the enthalpy values of the flow leaving the evaporator (h_d) reaching the delivery pressure (h_c)through an isentropic process as shown in Eq. (3) and Fig. 3.

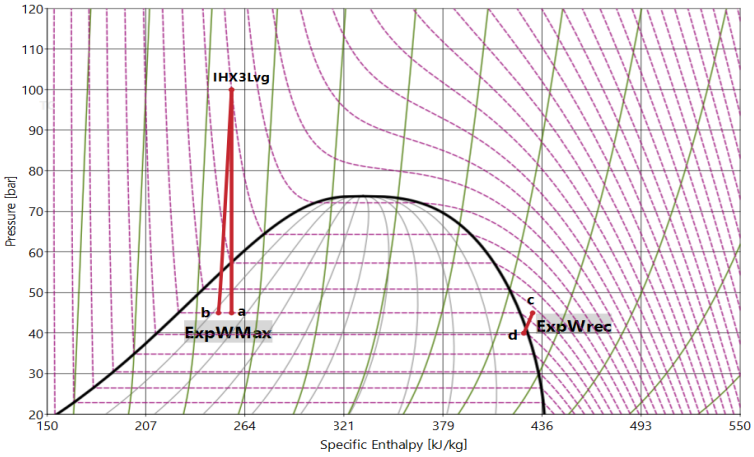

Figure 3 Ejector's expansion work recovery status

$$ExpW_{Rec} = h_c - h_d \quad \text{Eq. (3)}$$

where $ExpW_{Max}$ is maximum expansion work and it is calculated as the difference between the enthalpy values of the flow leaving the GC and reaching the delivery pressure through (h_a) isenthalpic and (h_b)isentropic processes respectively and stated in Eq. (4) and shown in Fig. 3.

$$ExpW_{Max} = h_a - h_b \quad \text{Eq. (4)}$$

By implementing the Bernoulli equation, the driving mass flow rate is evaluated using Eq. [5]

$$\dot{m}_{Dri} = A_{eff}\sqrt{2.\rho_{Dri}\,(P_{Dri} - P_{Suc})} \quad \text{Eq. (5)}$$

where ρ_{Dri} is the fluid density at the driving nozzle in kg·m^{-3}, A_{eff} is the effective cross area at the driving nozzle throat in m^2. The ejector mass balance equation Eq. (6) is defined as:

$$\dot{m}_{Del} = \dot{m}_{Suc} + \dot{m}_{Dri} \quad \text{Eq. (6)}$$

where $\dot{m}_{Del}, \dot{m}_{Suc}$ and $\dot{m}_{Dri}$ are the mass flow rates (kg·s^{-1}) through the delivery, suction and driving ports respectively.

The ejector energy balance equation Eq. (7) is defined as:

$$\dot{m}_{Dri}\,.h_{Dri} + \dot{m}_{Suc}.h_{Suc} = \dot{m}_{Del}.h_{Del} \quad \text{Eq. (7)}$$

where h_{Dri}, h_{Suc}, h_{Del} is the specific enthalpy of the driving, suction, and delivery ports (kJ.kg^{-1}) receptively.

For numerical modeling purposes, governing equations (1 to 7) are utilized in the TIL library to describe the ejector component model instantiated in the present study. A constant efficiency equal to 0.2 was assumed, as recommended by Hafner et al. (2014).

2.1.3. Thermal storage system

Maintaining the stratification within the four ways storage tanks is a key aspect in an efficient TES system and one of the design challenges, especially during high thermal demands. Implementing the in-series storage tanks has decreased the temperature gradient steep slope between the tanks' top and bottom levels and improved the system's thermal stratification, Smitt et al. (2020, 2021).

The indicated technique involves having the cold tank on one side (tank1), the hot tank on the other side (tank5), and in between some middle tanks where the bottom of tank5 is connected to the top of tank4 and so on until the coldest, tank1. It is important to highlight that these connections allow for a bi-directional

flow meaning that the water volume moves back and forth horizontally between the cold and hot tanks based on the charging and discharging status.

As shown in Fig. 1, the current system includes five in-series tanks, each of 3 m^3; the cold tank is connected to both the cold water CW source and the inlet of GC(2'), while the hot tank is connected to the outlet of GC(2) and the Domestic Hot water DHW hotel supply.

The stratified tank component model is instantiated from the MBL Modelica library, where the tank volume is discretized into a number of segments, i.e. in the present study, 10 segments were assumed. Eq. (8) evaluates the conduction heat flow between each fluid segment and the next one.

$$Q_{vol} = \frac{kA}{l} \left(T_{i+1} - T_i \right) \quad \text{Eq. (8)}$$

where Q_{vol} is the conduction heat flow between the current segment (i) and the next one (i+1), *k* is the water thermal conductance ($W \cdot m^{-1} \cdot K^{-1}$), *A* is the tank cross-sectional area (m^2), l is the volume segment height (m), T_i T_{i+1} water temperature of the current and following volume segments respectively. While Eq. (9) evaluates the enthalpic flow

$$EntFlow = \sum \dot{m}_W \, . \, h_{flow} \quad \text{Eq. (9)}$$

where, $\dot{m}_W$ is the sum of the water flow rate of all fluid ports connected to each mixing volume segment in ($kg \cdot s^{-1}$), i.e. entering (positive sign) and leaving (negative sign), i.e. according to the Modelica conventions MSL, h_{flow} is the enthalpy of the water flow in ($J \cdot kg^{-1}$).

The energy balance of each volume segment is evaluated from Eq. (10)

$$U_i = \int_{t_i}^{t} (Q_{vol} + EntFlow) \quad \text{Eq. (10)}$$

where, U_i is the volume segment's internal energy or the water storage energy due to the temperature changing from one timestep (t_i) to the next (t) in (J).

2.2. Recovering thermal storage tanks losses approach

The water storage system encounters thermal losses all day for different reasons, such as the conduction heat transfer to the ambient and low quality of stratification. However, during the charging-discharging processes, these losses become much less prominent.

The challenge appears during the standstill or night operation, i.e., very low or no DHW demands; the thermal losses cause the water temperature inside the storage tanks to drop. To recover this loss, an innovative approach allows the water coming from tank1, and subsequently heated through GC2' to be mixed with water from the upper level of tank2 via a three-way modulating valve (V3), as shown in Fig. 1. The mixture is connected to GC2 to reach the heating set point, while the input signal to activate the safety measurement is the water temperature entering GC2'. The approach stops the relatively hot water column migration to tank1 which will eventually increase its temperature above the threshold of 34˚C and force the heat pump

Author Accepted Manuscript version of the paper by Hagar Elarga et al.
in Proceedings of the 26th IIR International Congress of Refrigeration: Paris , France, August 21-25, 2023 - volume 4 (2023) p. 1105-1116,
http://dx.doi.org/10.18462/iir.icr.2023.0457

to stop. The three-way valve is controlled to allow the flow mixing only if the temperature difference between the flow leaving tank2 and GC(2') is equal to or lower than 5 K. This condition maximizes the system's exergy.

2.3. Numerical study features

2.3.1. Scenarios under investigation

A comparison between implementing the with (WTWV) and without (WOTWV) three-way valve approaches is executed to demonstrate the possibilities behind recovering thermal storage losses. The DHW daily consumption equals 21101.4 l/day, following a profile as represented in Figure 4. This information was obtained from a hotel installation from a partner in India at the project INDEE+. It is important to mention that cooling system is assumed to be working 24/7 as per the common practice at Indian hotels.

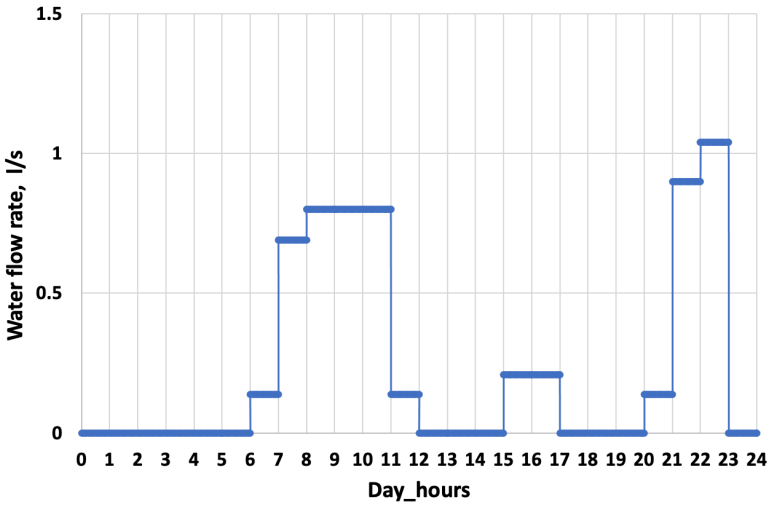

Figure 4 Daily DHW demands

2.3.2. TES Model Initial conditions

Uniform distribution and partially charged conditions are assumed for the TES system, as shown in Table 2 where the five tanks' initial water temperatures are illustrated.

Table2 TES initial conditions

Tank	1	2	3	4	5
Temperature ˚C	30	45	55	70	70

3. RESULTS

This section is subdivided into two parts; the first part discusses the CO_2 cycle performance, including the gas coolers, evaporators' thermal loads, and compressors' status. While the second part highlights the performance of the hydronic circuit, including thermal storage tanks and chilled water temperature, stratification quality, and three-way valve mass flow rate.

3.1. CO_2 heat pump chiller

At first glance, the CO_2 cycle's results did not demonstrate a significant difference between the two cases under investigation, the WTWV, and WOTWV. Fig. 5a and 5b illustrate the daily operating modes, with the

Author Accepted Manuscript version of the paper by Hagar Elarga et al.
in Proceedings of the 26th IIR International Congress of Refrigeration: Paris , France, August 21-25, 2023 - volume 4 (2023) p. 1105-1116,
http://dx.doi.org/10.18462/iir.icr.2023.0457

cooling mode ON all day, i.e., as assumed, while the heating mode is ON as a function of the tank's thermal charging status, with 30 min difference between the WTWV and WOTWV.

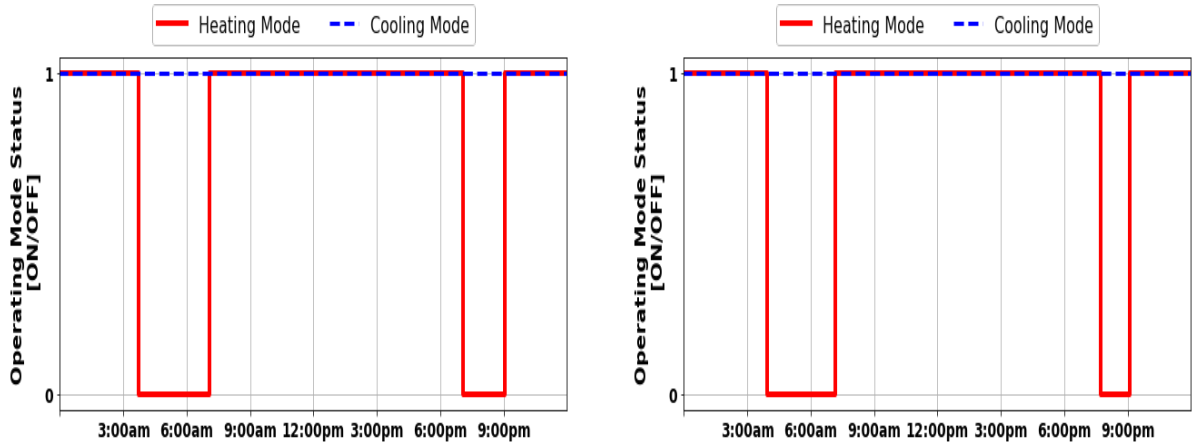

(a)WTWV case **(b)WOTWV case**

Figure5 System operational mode

Since both cases have the same heating and cooling loads, it was expected that the CO_2 cycle heat flow profiles to be similar as shown in Fig. 6a and 6b, apart from brief performance instabilities induced by staging the conFCom up and down in case of the WOTWV. The average heat flow of both gas coolers and evaporators is 52 kW and 40 kW, respectively.

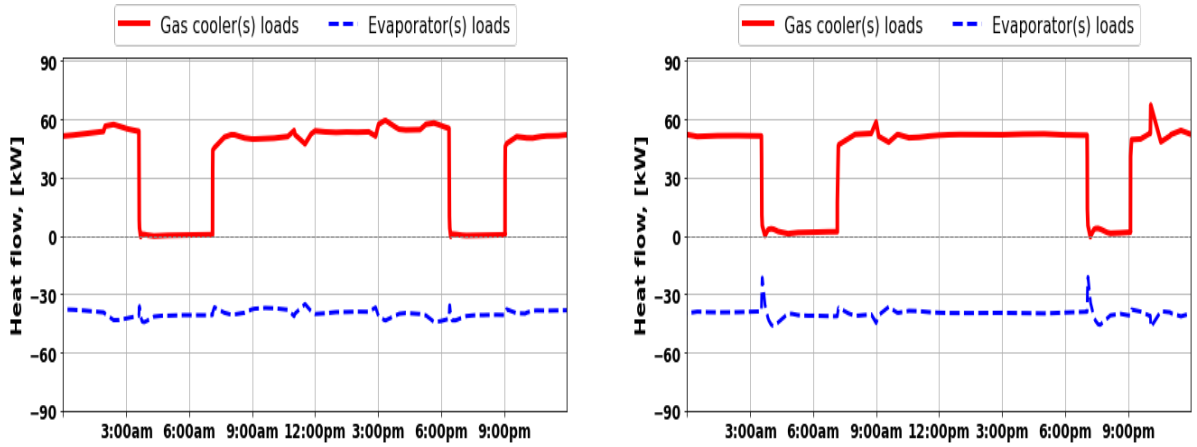

(a) (b)

Figure6 CO_2 system Gas Cooler(s) and Evaporator(s) heat flow; a) WTWV , b) WOTWV

The essential difference between the two scenarios lies mainly within the condition that triggered the heating charging to stop each case. In the WTWV case, the charging stops because the tanks have reached the design setpoint temperatures without resorting to the system safety measurement. While in the WOTWV case, the temperature of the water entering (GC2') has reached 34˚C plus the hysteresis, which motivates the thermal charging process to stop, and the refrigerant is diverted to the air-cooled gas cooler (GC2"), as shown in Fig. 7.

Author Accepted Manuscript version of the paper by Hagar Elarga et al.
in Proceedings of the 26th IIR International Congress of Refrigeration: Paris , France, August 21-25, 2023 - volume 4 (2023) p. 1105-1116,
http://dx.doi.org/10.18462/iir.icr.2023.0457

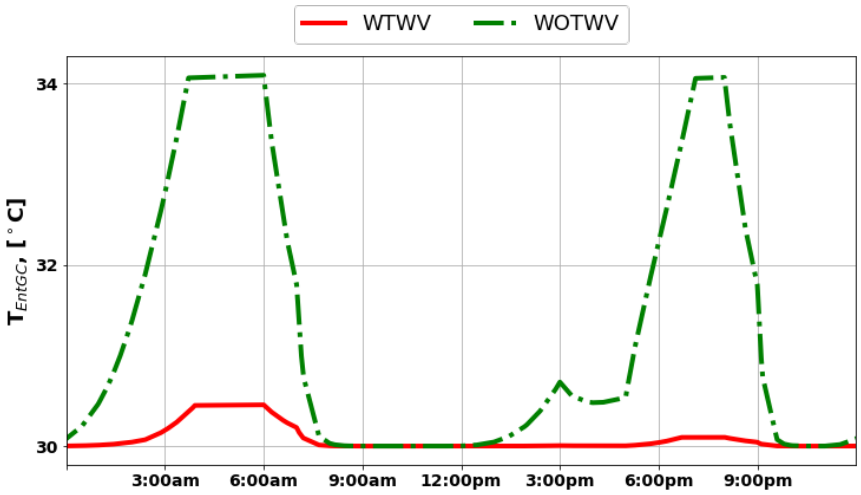

Figure7 GasCooler2' entering water temperature

The influence of having a higher GC(2') entering water temperature TEntGC value was not limited to compromising the thermal charging efficiency, but rather it reduced the system COP by raising the compressor's electrical consumption of the WOTWV 12 kW with a daily energy consumption of 397 kWh compared to the WTWV with 385 kWh and 3% savings.

3.2. Chilled and heating circuits

Fig. 8, i.e. from 8a to 8j demonstrates the daily vertical temperature distribution of the TES system ordered ascending from tank1 to tank5, with the WTWV on the left side and WOTWV on the right side. It was noticed that the quality of the charging process and the stratification across the storage tanks were higher for the former case than the latter. For the WTWV case, the maximum water temperature recorded for tank1 in Fig. 8a was 40.5 ˚C at the top level, while for the WOTWV case tank1 (Fig. 8b), the maximum water temperature reached 45 ˚C. By moving toward the hot tanks, it was observed that the water temperature of the WTWV case at tanks2, 3, and 4 is approaching the setpoint temperature of 70 ˚C even with the two DHW demands peaks occurring between 6:00 am and 12:00 pm and 8:00 pm to 11:00 pm, respectively. Tank5 is the first interaction with the hotel DHW demands and has remained fully charged all day in the case of the WTWV. While in the WOTWV case, its bottom level has lost about 7% of its charging capacity.

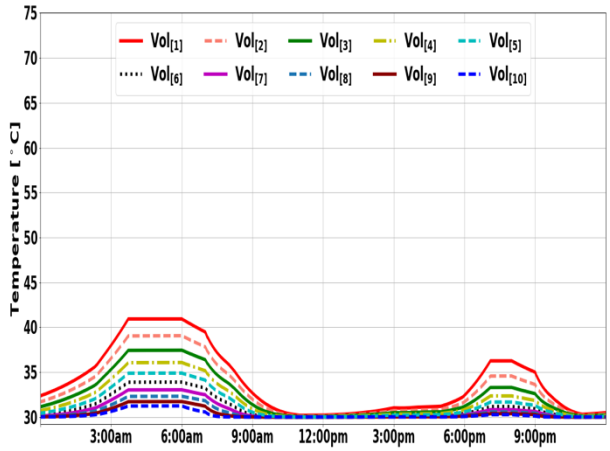

(a)WTWV-Tank1

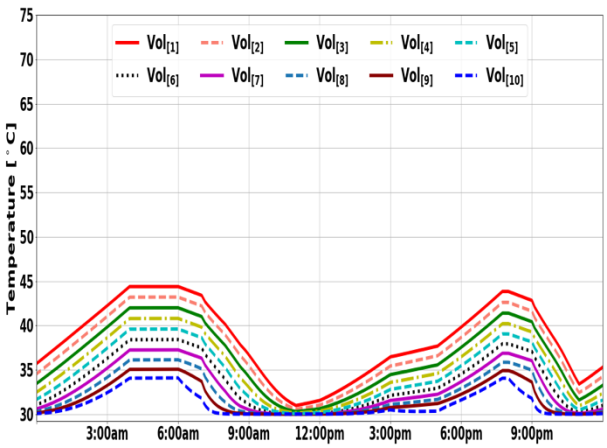

(b) WOTWV-Tank1

Author Accepted Manuscript version of the paper by Hagar Elarga et al.
in Proceedings of the 26th IIR International Congress of Refrigeration: Paris , France, August 21-25, 2023 - volume 4 (2023) p. 1105-1116,
http://dx.doi.org/10.18462/iir.icr.2023.0457

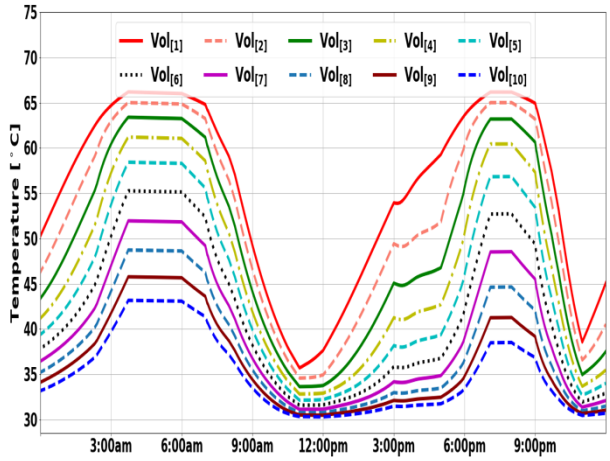

(c) WTWV-Tank2

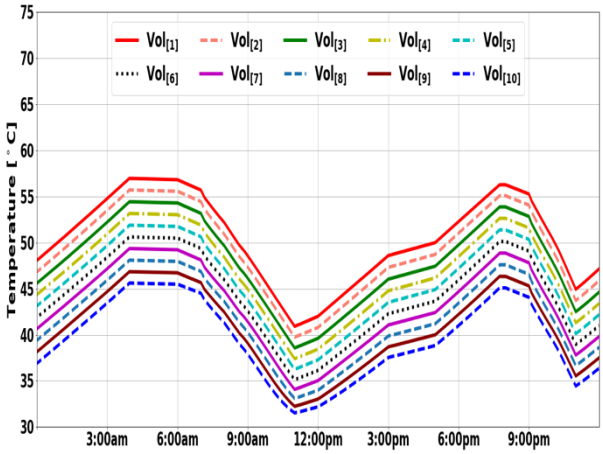

(d) WOTWV-Tank2

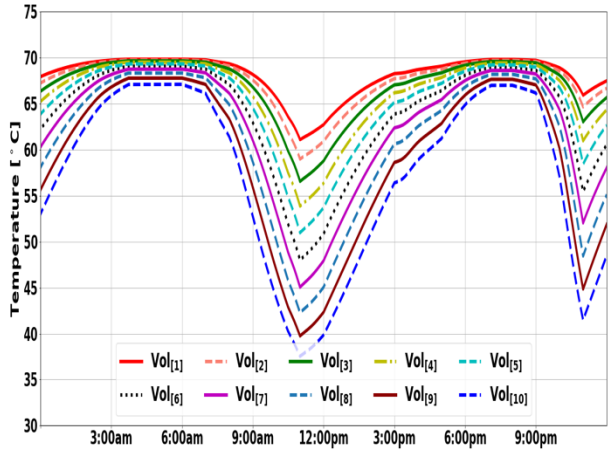

(e) WTWV-Tank3

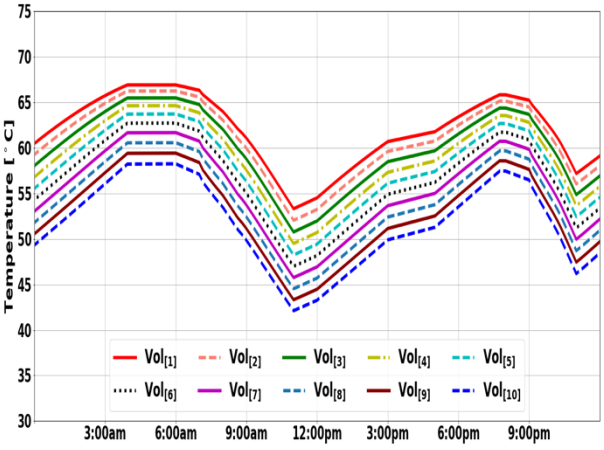

(f) WOTWV-Tank3

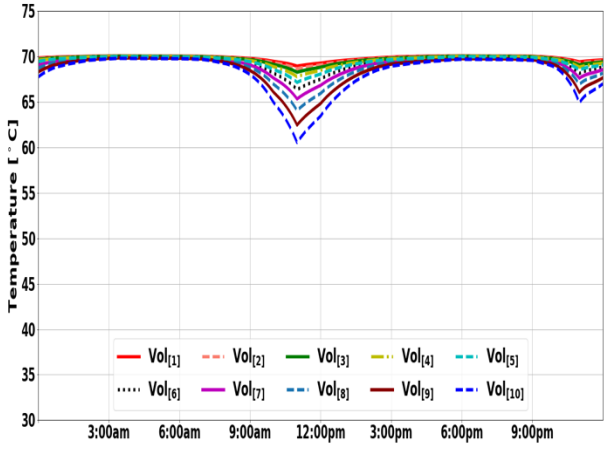

(g) WTWV-Tank4

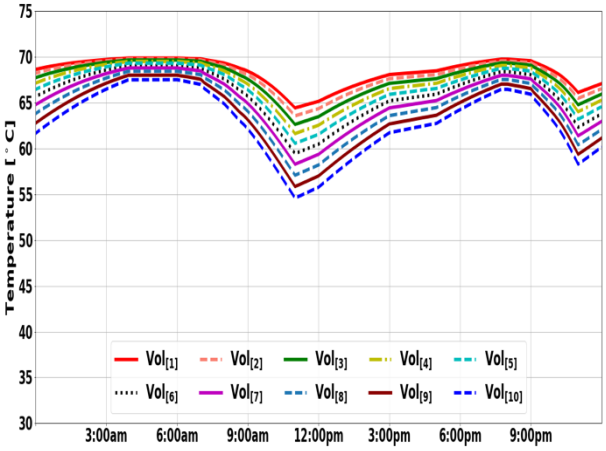

(h) WOTWV-Tank4

Author Accepted Manuscript version of the paper by Hagar Elarga et al.
in Proceedings of the 26th IIR International Congress of Refrigeration: Paris , France, August 21-25, 2023 - volume 4 (2023) p. 1105-1116,
http://dx.doi.org/10.18462/iir.icr.2023.0457

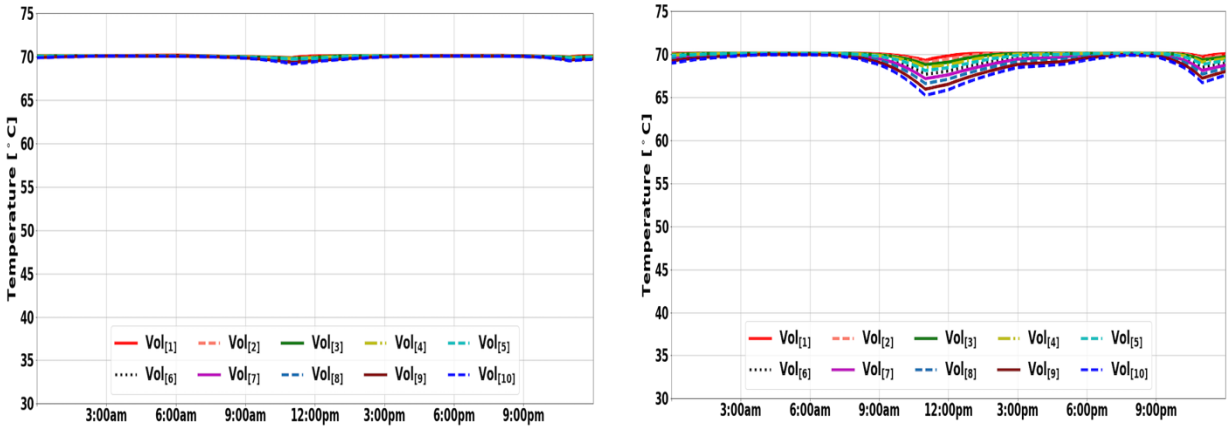

(i) WTWV-Tank5 **(j) WOTWV-Tank5**

Figure8 TES tanks stratification temperature profiles

4. CONCLUSIONS

The thermal recovery approach via a three-way valve is a simple method to improve the overall CO_2 system, support the harmonic operation between different components and raise the efficiency of the thermal charging process. Meanwhile, the user does not need expensive components; the thermal recovery approach enforces the control algorithm to correctly correspond to the design criteria, not resort to the system safety measures and failing to fulfill its design role.

The improvement in the TES stratification efficiency assures a:

1- higher CO_2 system COP, as the water entering GC(2'), is maintained within the acceptable limits, and the CO_2 unit shutdown safety measure is never reached.

2- better thermal charging/discharging performance, as the heating mode remains active until the charging status of the thermal tank set is fulfilled.

It is clearly shown that the charging/discharging efficiency is much better after utilizing the approach of mixing the two water streams leaving tank2 and GC(2'). On the other hand, the parallel control of the modulating three-way valve allows for faster thermal charging during both the standstill and high DHW demands. The future investigation shall include different boundary conditions and different models of the two-phase ejector.

ACKNOWLEDGEMENTS

The authors gratefully acknowledge the financial support of the Norwegian Ministry of Foreign Affairs (MFA) through the project of INDEE+.

REFERENCES

Artuso, P., Tosato, G., Rossetti, A., Marinetti, S., Hafner, A., Banasiak, K. and Minetto, S., 2021. Dynamic Modelling and Validation of an Air-to-Water Reversible R744 Heat Pump for High Energy Demand Buildings. *Energies*, *14*(24), p.8238.

Austin, B.T. and Sumathy, K., 2011. Transcritical carbon dioxide heat pump systems: A review. *Renewable and Sustainable Energy Reviews*, *15*(8), pp.4013-4029.

Cui, Q., Wang, C., Gao, E. and Zhang, X., 2022. Pinch point characteristics and performance evaluation of CO2 heat pump water heater under variable working conditions. Applied Thermal Engineering, 207, p.118208.

Dai, B., Zhao, X., Liu, S., Yang, Q., Zhong, D., Hao, Y. and Hao, Y., 2020. Energetic, exergetic and exergoeconomic assessment of transcritical CO2 reversible system combined with dedicated mechanical subcooling (DMS) for residential heating and cooling. Energy Conversion and Management, 209, p.112594.

David, A., Mathiesen, B.V., Averfalk, H., Werner, S. and Lund, H., 2017. Heat roadmap Europe: large-scale electric heat pumps in district heating systems. Energies, 10(4), p.578.

Elarga, H., Selvnes, H., Sevault, A. and Hafner, A., 2022. Numerical investigation of a CO2 cooling system connected to Spawn-of-Energy-Plus thermal zones. Applied Thermal Engineering, p.119908.

Elarga, H. and Hafner A., 2022. CO2 heat pump/chiller system for a hotel in a tropical climate: a numerical investigation. Proceeding of the 15th IIR Gustav Lorentzen Natural Working Fluids Conference, Trondheim, Norway, IIF/IIR.

Hafner, A., Försterling, S. and Banasiak, K., 2014. The multi-ejector concept for R-744 supermarket refrigeration. International Journal of Refrigeration, 43, pp.1-13.

INDEE+ project: https://www.ntnu.edu/indee/indee

Lorentzen, G. and Pettersen, J., 1993. A new, efficient and environmentally benign system for car air-conditioning. International journal of refrigeration, 16(1), pp.4-12.

Minetto, S., Condotta, M., Rossetti, A., Girotto, S. and Del Col, D., 2016. Ejector CO2 heat pump for space heating and cooling. In the proceedings of the 12th IIR Gustav Lorentzen Natural Refrigerants Conference, Edinburgh, Scotland, IIF/IIR.

MBL Modelica Buildings Library https://simulationresearch.lbl.gov/modelica/

MSL Modelica Standards library https://github.com/modelica/ModelicaStandardLibrary.

Pardiñas, Á.Á., Hafner, A. and Banasiak, K., 2018. Novel integrated CO2 vapor compression racks for supermarkets. Thermodynamic analysis of possible system configurations and influence of operational conditions. Applied Thermal Engineering, 131, pp.1008-1025.

Smitt, S., Tolstorebrov, I. and Hafner, A., 2020. Integrated CO2 system with HVAC and hot water for hotels: Field measurements and performance evaluation. International Journal of Refrigeration, 116, pp.59-69.

Smitt, S., Tolstorebrov, I. and Hafner, A., 2021. Performance improvement of integrated CO2 systems with HVAC and hot water for hotels. Thermal Science and Engineering Progress, 23, p.100869.

TLK-Thermo GmbH, 2020a. TIL Suite – Simulates thermal systems, https://www.tlk-thermo.com/index.php/en/software/38-til-suite.

Yamaguchi, S., Kato, D., Saito, K. and Kawai, S., 2011. Development and validation of static simulation model for CO2 heat pump. International Journal of Heat and Mass Transfer, 54(9-10), pp.1896-1906.

Ye, Z., Wang, Y., Zendehboudi, A., Hafner, A. and Cao, F., 2022. Investigation on the performance of fluted tube-in-tube gas cooler in transcritical CO2 heat pump water heater. *International Journal of Refrigeration*, *135*, pp.208-220.